SUPPLEMENTARY FIGURES

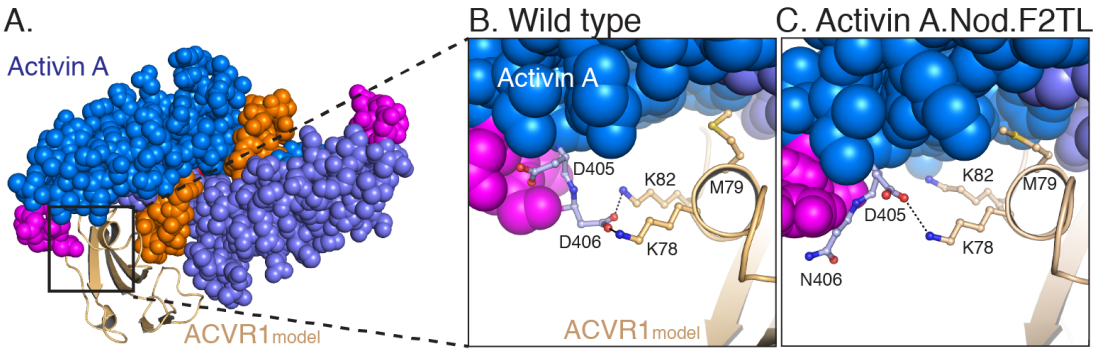

Supplemental figure 1: Model of Activin A:ACVR1 structure

A) Activin A from its structure with Follistatin 288 (2BOU) {Thompson, 2005} was aligned into GDF11 structure from its ternary complex with TGFBR1 and ACVR2B (6MAC) {Goebel et al, in review}. The Acvr1 model was aligned to TGFBR1 in the TGFBR1:GDF11:Acvr2B complex to give the energy minimized model (A). B) Closer examination of the F2TL interaction in this model clearly shows Activin A F2TL residue D406 interacting electrostatically with both ACVR1 residues K78 and K82. C) Substitution of Nodal F2TL into Activin A shows that F2TL coordination is disrupted.

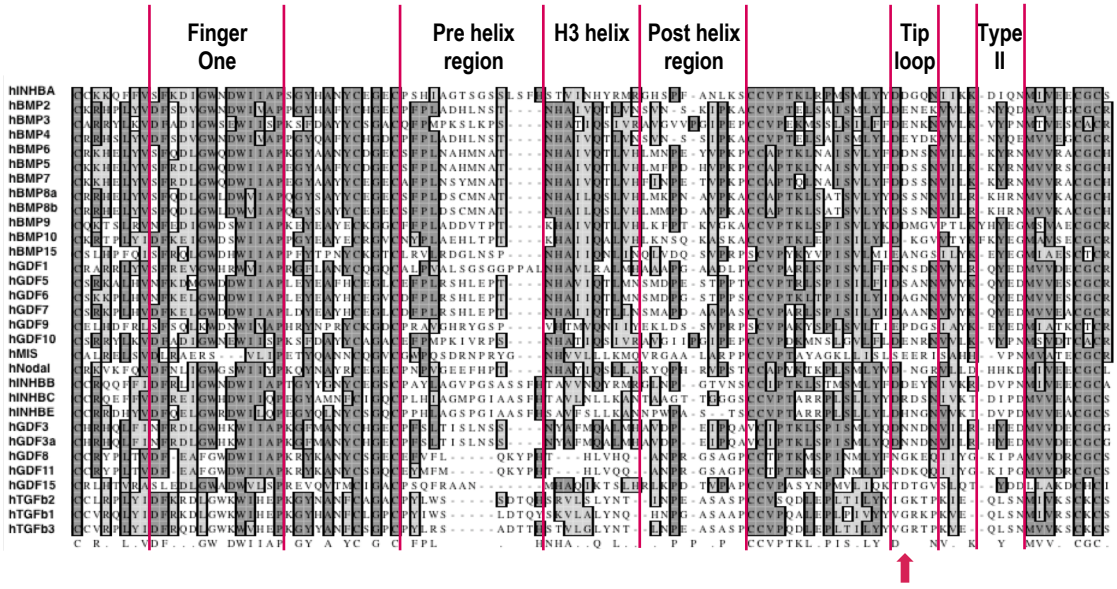

Supplemental figure 2: Sequence alignment of mature ligands in human TGFβ family
Sequences of human TGFβ family of mature ligands were aligned in MacVector with ClustalW. Structural elements involved in receptor binding are highlighted as follows; finger one, pre-helix region, H3 helix (central helix), post-helix region, tip loop (F2TL), and site of sequence diversity coding for type II receptor binding specificity (type II). Looking for regions of sequence diversity within the family, the pre and post-helix regions and F2TL were chosen for substitutional mutagenesis analysis of Activin A. Position 406 is marked with a red arrow.

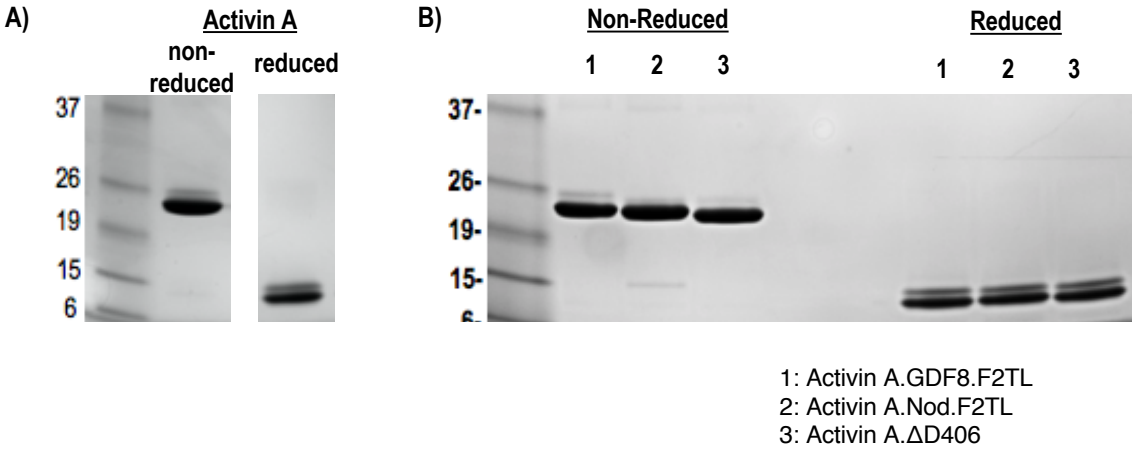

Supplemental figure 3: Purified Activin and and Activin A F2TL muteins

Activin A was purified from CHO-K1 cell supernatants by heparin affinity and ion exchange chromatography. The mature form of Activin A and Activin A muteins was separated by reverse phase chromatography, and products were analyzed by Coomassie blue stained SDS-PAGE gels. Activin A (A) and Activin A F2TL muteins (B) are shown under reducing and non-reducing conditions.

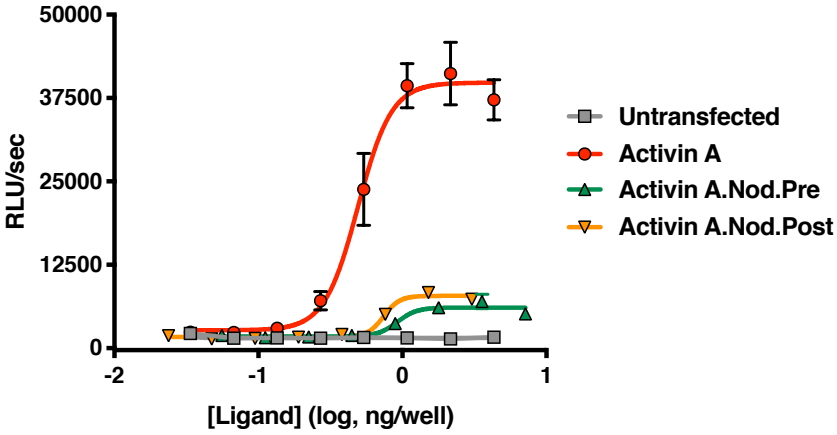

Supplemental figure 4: Activin A with pre-helix and post-helix substitutions from Nodal have reduced ability to activate the Smad 2/3 pathway.

Supernatants from CHO cells expressing Activin A with the pre or post-helix sequence from human Nodal were tested for activity in HEK293 Smad 2/3 reporter cells. Both the Activin A.Nod.Pre and Activin A.Nod.Post supernatants have reduced activity compared to Activin A (R&D Systems).

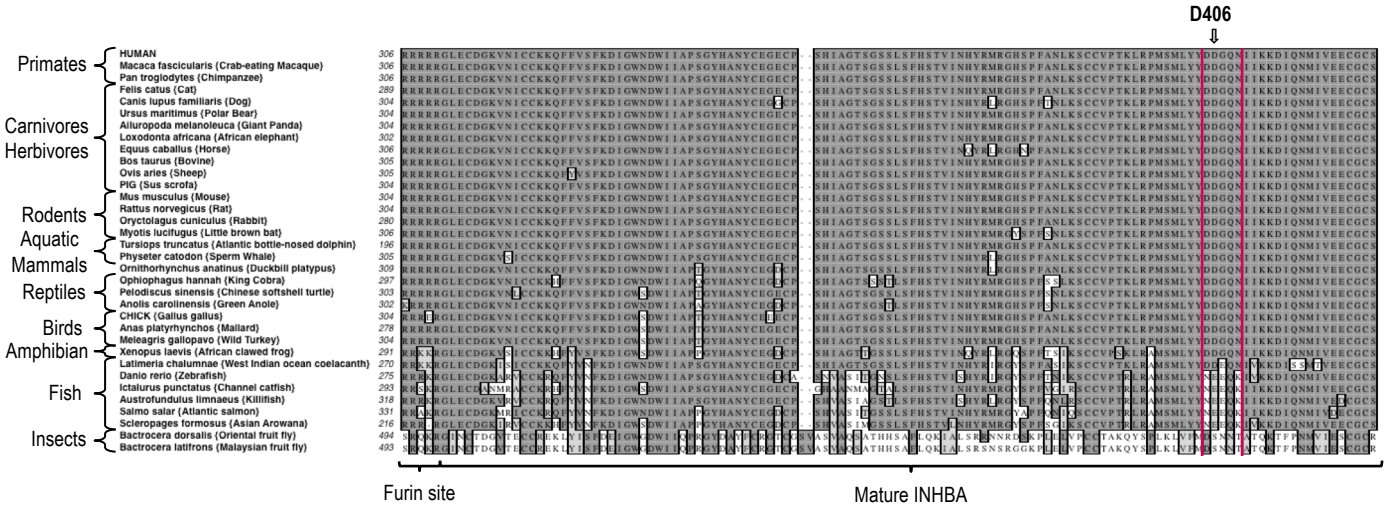

Supplemental figure 5: Sequence alignment of Activin A from various species

A Clustal W alignment with the F2TL sequence bracketed in red. Human Activin A aspartic acid at position 406, D406, is evolutionarily well conserved in vertebrates. We see divergence of this sequence in most fish species.

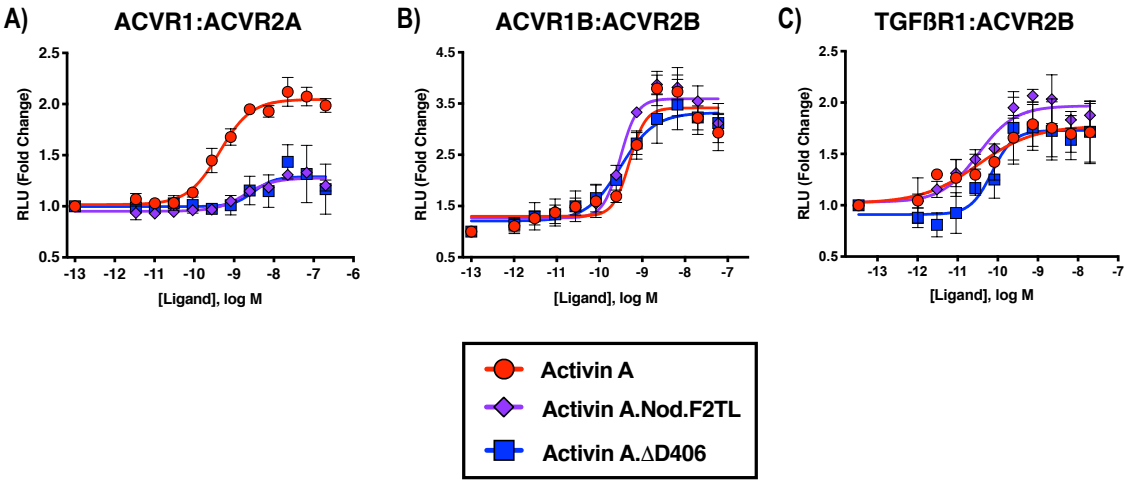

Supplemental figure 6: Activin A F2TL muteins lose binding to Acvr1.
U20S cells expressing split beta-galactosidase fusions of corresponding type I and type II receptors were treated with a dose response of Activin A ligands. Type 1 receptor binding was measured by luminescence. The finger two tip loop mutants have reduced ability to dimerize ACVR1:ACVR2A receptors, while retaining wild type capacity to dimerize ACVR1B:BMPR2 and TGFβR1:ACVR2B receptor pairs.

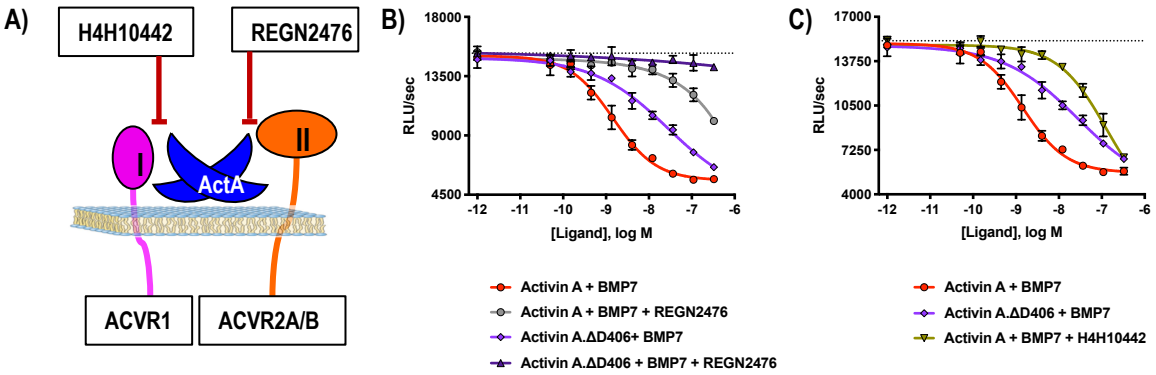

Supplemental figure 7: Activin A.ΔD406 has reduced antagonism of Smad1/5/8 signaling

Activin A.ΔD406 shows reduced antagonism of BMP7 signaling to Smad 1/5/8. Varying concentrations of Activin A or Activin A.ΔD406 were mixed with a constant concentration of BMP7 (12nM) and applied to HEK293 cells stably transfected with the Smad1/5/8 reporter construct driving firefly luciferase. A) Schematic showing H4H10442 blocking activin binding to Type I receptor and REGN2476 preventing binding to Type II receptor. B) Using REGN2477 we show the remaining inhibition of BMP7 by Activin A.ΔD406 is lost when binding to Type II receptor is blocked. C) Inhibition of type I receptor binding of wild-type Activin A shows an increased reduction in BMP inhibition compared to Activin A.ΔD406 alone. Inhibition of BMP7 is reduced ~ 15 fold with Activin A.ΔD406 compared to 60 fold with the Activin A:H4H10442 complex. (The IC_{50}s of Acitivin A and Activin A.ΔD406 are 1.4×10^{-9} M and 2.0×10^{-8} M, respectively.)

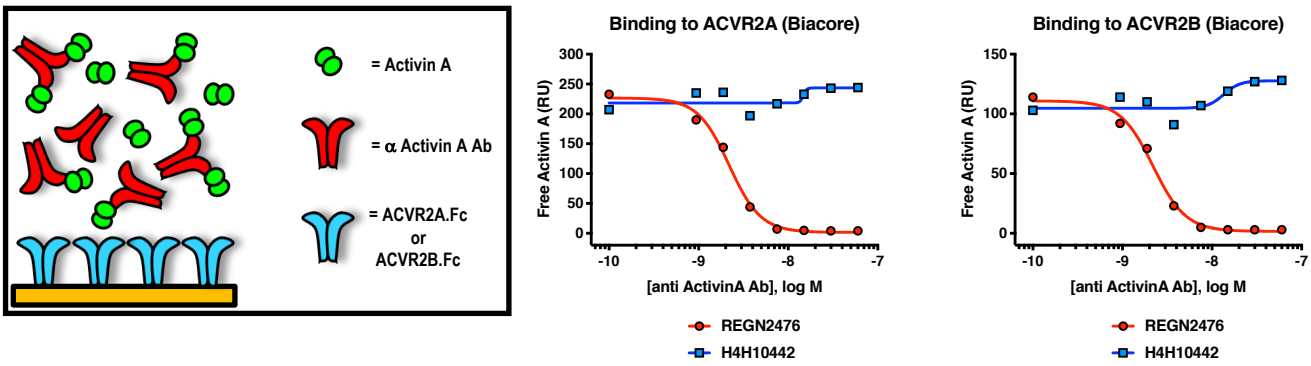

Supplemental figure 8: Anti-Activin A antibody REGN2476 blocks binding of Activin A to type II receptors ACVR2A and ACVR2B. Anti-Acivin A antibody H4H10442 and REGN2476 at concentration range 0.94 nM-60 nM were pre-mixed with 5nM Activin A and injected over A) Acvr2A or B) Acvr2B Fc fusion protein coupled chip surfaces. Anti-Activin A antibody H4H10442 allows binding to ACVR2A and ACVR2B surfaces. REGN2476 directly blocks Activin A binding to both type II receptors.

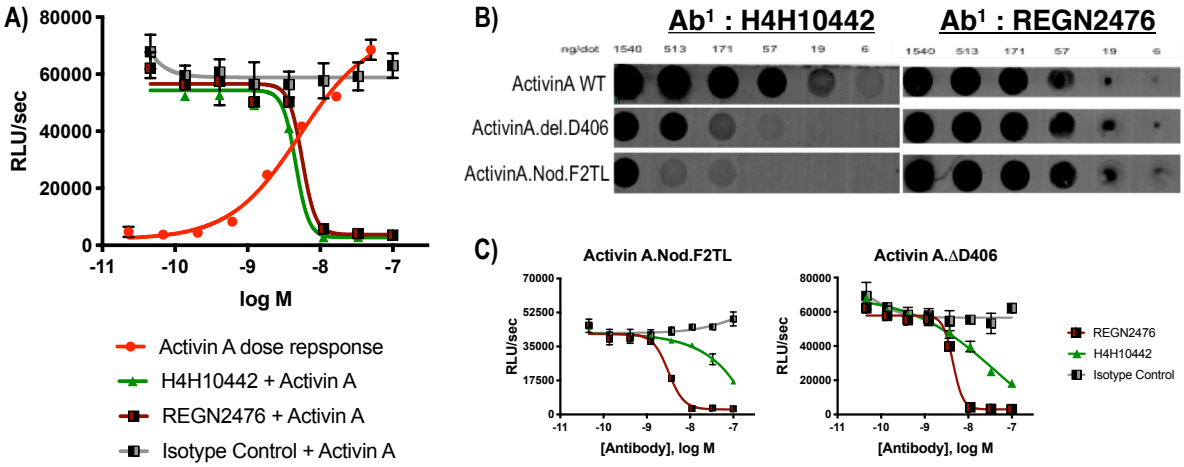

Supplemental figure 9: Activin A antibodies REGN2476 and H4H10442 block signaling but bind Activin A at two different sites

A) Both H4H10442 and REGN2476 anti-Activin A antibodies block Activin A (10nM) signaling to Smad2/3 pathway in HEK293 CAGA-luciferase reporter cells. B) For dot blots, purified Activin A and Activin A muteins were serially diluted and applied to PVDF membranes using suction. Membranes were blocked using Odyssey blocking reagent and the hIGg4 was visualized using a IRDye 680RC conjugated goat anti-human secondary antibody (Li-cor). REGN2476 bound similarly to all three Activin A preparations. However, loss of binding of H4H10442 to the F2TL muteins of Activin A suggests binding at this type I receptor binding site. C) In HEK293 Samd2/3 luciferase reporter cells, H4H10442 is a less effective inhibitor of the Activin A F2TL muteins (10 nM) when compared to wild type Activin A.

A)

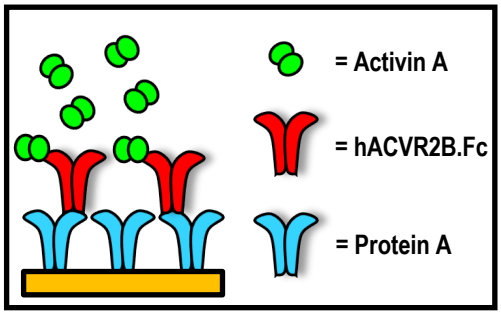

B)

Capture Surface	Dimer Captured (RU)	Reagent Tested	100nM Reagent Bound (RU)	ka (1/Ms)	kd (1/s)	KD (M)	t½ (min)
hACVR2B.hFc	117 ± 0.7	rh/m/r Activin A (R&D)	31	9.98E+06	2.03E-04	2.03E-11	57
	118 ± 1	ActivinA WT	33	2.13E+07	2.24E-04	1.05E-11	52
	117 ± 0.9	ActA.Nod.F2TL	33	5.29E+07	2.70E-04	5.11E-12	43
	116 ± 0.8	ActA.delta.D406	33	5.50E+07	2.54E-04	4.62E-12	46

Supplemental figure 10: Activin A finger 2 tip loop muteins do not alter type II receptor binding.

A) Schematic representation of surface plasmon resonance binding assay. B) Binding of mature Activin A and Activin A mutein protein to Protein A captured ACVR2B Fc. Mutations to Activin A F2TL do not disturb type II receptor binding site.

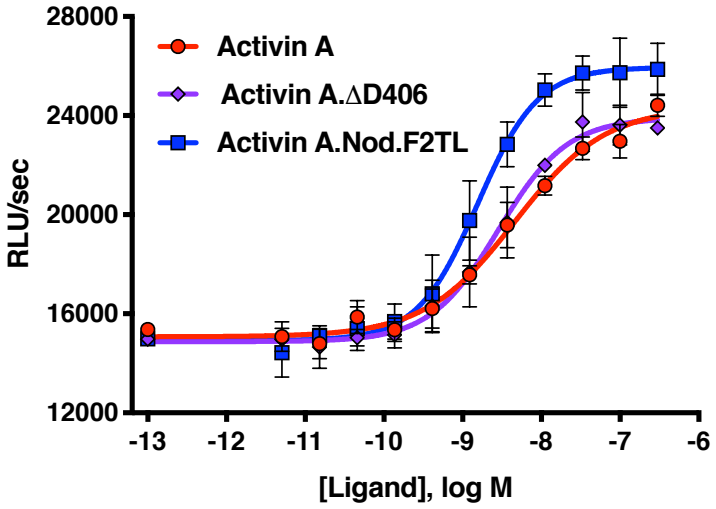

Supplemental figure 11: Activin A F2TL muteins can signal through ACVR1[R206H] like wild type Activin A

HEK293 cells expressing FOP mutant Acvr1 (Acvr1[R206H]) were treated with a dose response of Activin A ligands. Even though Activin A F2TL muteins have reduced binding to ACVR1, they continue to signal to Smad1/5/8 pathway via ACVR1[R206H] receptor in the BRE-luciferase reporter assay.

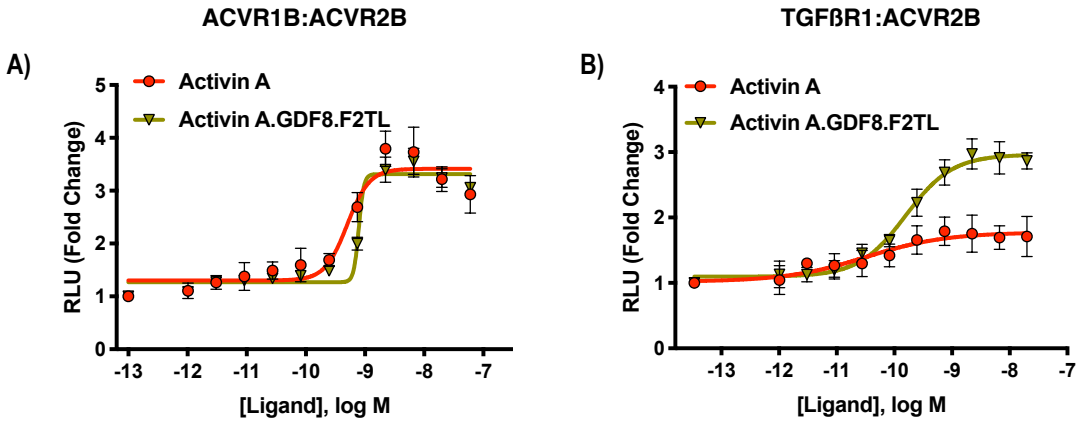

Supplemental Figure 12: Activin A.GDF8.F2TL mutein binds TGFβR1 better than Activin A
U20S cells expressing split beta-galactosidase fusions of corresponding type I and type II receptors were treated with a dose response of Activin A.GDF8.F2TL and Activin A. Type 1 receptor binding was measured by luminescence in these receptor dimerization assays. A) Activin A.GDF8.F2TL retains wild type capacity to dimerize ACVR1B:BMPR2, and Activin A.GDF8.F2TL increases dimerization of the TGFBR1:ACVR2B receptor pairs (B).

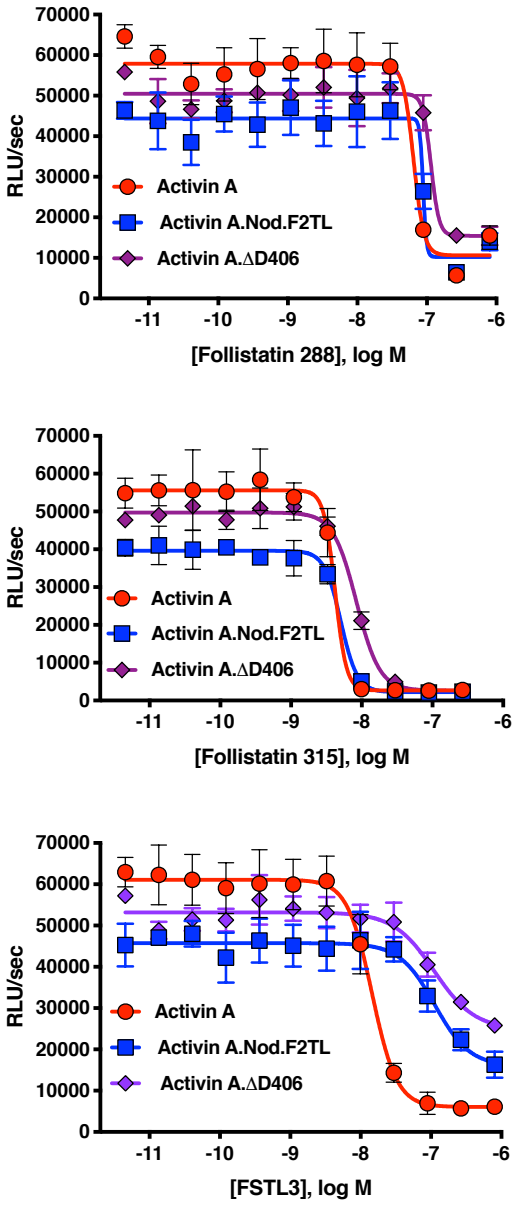

Supplemental Figure 13: Activin A.Nod.F2TL mutein is inhibited by Follistatin but shows reduced inhibition by FSTL3

Varying concentrations of Follistatin and FSTL3 were preincubated with a constant concentration of Activin A, ActivinA.Nod.F2TL or ActivinA.del.D406 (10nM). Activity was tested in HEK293 cells harboring the Smad2/3 luciferase reporter. Activity of Activin A, ActivinA.Nod.F2TL and ActivinA.del.D406 was blocked by both follistatin-288 (A) and follistatin-315 (B). (C) FSTL3 is a less effective inhibitor of ActivinA.Nod.F2TL and ActivinA.del.D406 when compared to wild-type Activin A.